

Article

Leaching of Metal Ions from Blast Furnace Slag by Using Aqua Regia for CO₂ Mineralization

Jun-Hwan Bang, Seung-Woo Lee, Chiwan Jeon, Sangwon Park, Kyungsun Song, Whan Joo Jo and Soochun Chae *

CO₂ Sequestration Department, Korea Institute of Geoscience and Mineral Resources (KIGAM), 124 Gwahang-no, Yuseong-gu, Daejeon 34132, Korea; jhbang@kigam.re.kr (J.-H.B.); swlee21th@kigam.re.kr (S.-W.L.); jcw@kigam.re.kr (C.J.); psw1231@kigam.re.kr (S.P.); kssong@kigam.re.kr (K.S.); chohwanju@kigam.re.kr (W.J.J.)

* Correspondence: chae@kigam.re.kr; Tel.: +82-42-868-3659; Fax: +82-42-868-3421

Academic Editor: Vijay Kumar Thakur

Received: 5 September 2016; Accepted: 23 November 2016; Published: 25 November 2016

Abstract: Blast furnace slag (BFS) was selected as the source of Ca for CO₂ mineralization purposes to store CO₂ as CaCO₃. BFS was dissolved using aqua regia (AR) for leaching metal ions for CO₂ mineralization and rejecting metal ions that were not useful to obtain pure CaCO₃ (as confirmed by XRD analysis). The AR concentration, as well as the weight of BFS in an AR solution, was varied. Increasing the AR concentration resulted in increased metal ion leaching efficiencies. An optimum concentration of 20% AR was required for completely leaching Ca and Mg for a chemical reaction with CO₂ and for suppressing the leaching of impurities for the production of high-purity carbonate minerals. Increasing the liquid-to-solid ratio (L/S) resulted in the increased leaching of all metal ions. An optimum L/S of 0.3/0.03 (=10) was required for completely leaching alkaline-earth metal ions for CO₂ mineralization and for retaining other metal ions in the filtered residue. Moreover, the filtrate obtained using 20% AR and an L/S of 0.3/0.03 was utilized as Ca sources for forming carbonate minerals by CO₂ mineralization, affording CaCO₃. The results obtained herein demonstrated the feasibility of the use of AR, as well as increasing pH, for the storage of CO₂ as high-purity CaCO₃.

Keywords: blast furnace slag; CO₂ mineralization; calcium leaching

1. Introduction

CO₂ mineralization or carbonate mineralization is an alternative approach to store anthropogenic CO₂, which can be transformed into carbonate minerals, such as calcium carbonate (CaCO₃) and magnesium carbonate (MgCO₃), via a chemical reaction with alkaline-earth metal ions; these metal ions can be obtained from natural minerals [1], industrial by-products, and wastes [2,3]. Mineralization can be broadly categorized into two methods: direct mineralization, in which CO₂ directly reacts with sources of alkaline-earth metal ions, and indirect mineralization, in which CO₂ indirectly reacts in an aqueous phase with the metal ions which are introduced by additional treatment before conducting the main reaction in situ [4,5]. Typically, for CO₂ mineralization, the pH needs to be increased to greater than 10.3 for the ionization of CO₂ to CO₃²⁻ for facile combination with metal ions (in an aqueous phase) [6]. In addition, other procedures are employed for the ionization of alkaline-earth metal ions to facilitate combination with CO₃²⁻ [3,7–11].

Alkaline-earth metal ions present in natural minerals are ionized at high temperature and pressure, as well as by reagents, such as acids and alkalis. Kleive and Thornhill [12] have pretreated a natural mineral such as olivine, which enhances its reactivity with CO₂, followed by chemical treatment, and reported that the concentrations of leached Mg and Fe increase with increasing acid concentration. Huijgen et al. [13] have reported that wollastonite (CaSiO₃) can be used as a metal

source for CO₂ mineralization; wollastonite was powdered, added into an autoclave, and subjected to high temperature and high CO₂ pressure for direct mineralization. As a result, nearly 40% of the Ca present in wollastonite is converted to CaCO₃. Nduagu et al. [14] have used Finnish serpentinite to leach Mg ion by using (NH₄)₂SO₄ and formed Mg(OH)₂ by using aqueous ammonia. As compared to the mother minerals, Finnish serpentinite, Mg(OH)₂ is more reactive toward CO₂. Based on the procedures for leaching Mg and forming Mg(OH)₂, the authors [15] have also tested various Mg silicate rocks from Finland, Lithuania, Australia, and Norway. They found that the amount of metal ions leached from these rocks vary with mineral locations. Mg ion in the aqueous phase was also used as metal ion source for CO₂ mineralization. A magnesium chloride (MgCl₂·6H₂O) solution was prepared to synthesize nesquehonite (MgCO₃·3H₂O) [16–19] and to study phase transitions from nesquehonite to dypingite (Mg₅(CO₃)₄(OH)₂·5H₂O) [20]. Hopkinson et al. have reported a more detailed study on the phase transitions for magnesium carbonates [21].

Eloneva et al. [22] have reported that blast furnace slag (BFS), the byproduct obtained from the steelmaking process, is useful for CO₂ mineralization. First, BFS (50 g) was suspended in 1 L of a 20% acetic acid solution (~pH 4), and then the precipitate and silica gel were separated after the reaction. Acid was removed by heat treatment at 423–433 K for retaining alkali calcium acetate. The separated precipitate was suspended in deionized (DI) water with a NaOH solution (50 wt %) for rendering conditions favorable for CO₂ mineralization. Based on their study, Chiang et al. [23] have conducted two-step experiments for the selective leaching of Ca: First, 100 g of BFS was suspended in 731 mL of an acid solution at concentrations of 0.5–2 M. Second, the suspension was treated with CO₂ after heating and stirring for 1 h. Using a 2 M acetic acid solution containing BFS, the leaching efficiencies of Al, Ca, Mg, and Si were 38%, 90%, 100%, and 7%, respectively, after the second leaching. Ammonium chloride was also used as the leaching agent for Ca from basic oxygen steelmaking debris, secondary steelmaking slag, and hot metal desulfurization slag [24]. Hall et al. have added the abovementioned slags in a 2 M ammonium chloride solution and utilized them for leaching Ca at a leaching time of 2 h. The leaching efficiency of Ca ranges from 24% to 38% for a slag particle size of less than 150 μm. They also demonstrated the possibility of synthesizing zeolites from the leached residues. Eloneva et al. have investigated the use of various ammonia leaching agents, such as ammonium acetate (CH₃COONH₄), ammonium nitrate (NH₄NO₃), and ammonium chloride (NH₄Cl), for the leaching of Ca from 100 g of steel converter slag for precipitating high-purity CaCO₃ [25]. Recently, Lee et al. have used several ammonium salts (e.g., NH₄NO₃, NH₄Cl, CH₃COONH₄, and (NH₄)₂SO₄) for leaching Ca from BFS at ambient temperature and pressure [26] and examined the leaching efficiency of Ca with respect to the types and concentration of solvents, temperature, reaction time, and solid-to-liquid ratio (S/L). With increasing solvent concentration, temperature, and reaction time, the Ca leaching efficiency increases to near 52 wt %. Meanwhile, S/L does not proportionally increase the Ca leaching efficiency.

Several studies have primarily reported the use of strong or weak acids for leaching alkaline-earth metal ions [8,27–29] from various steelmaking slags. Acid solution strength exhibits both advantages and disadvantages for leaching. Typically, although a strong acid is efficient for leaching Ca, large amounts of other metal ions, such as Fe or Mn, present in slag can also be leached. Furthermore, the use of a strong acid requires a large amount of alkali to neutralize the reactant phases for rendering conditions favorable for CO₂ mineralization. In contrast, although weak acids or even bases are not suitable for leaching Ca, marginal amounts of alkali are required for rendering conditions favorable for CO₂ mineralization. In this study, BFS and aqua regia (AR) were selected as the source of alkaline-earth metal ions and leaching agent, respectively, for CO₂ mineralization. To the best of our knowledge, AR has not been used as a leaching agent in CO₂ mineralization. As a type of strong acid, AR is known to exhibit a strong oxidizing ability toward various metal ions, such as Ca, Mg, and Fe, and is non-corrosive to silica. Moreover, the effects of the variation of AR concentration and liquid-to-solid ratio (L/S; volume of AR solution/weight of slag) on the leaching efficiency of metal ions from BFS were investigated. In addition, experiments were conducted for the selective leaching of metal ions under the given leaching conditions.

2. Materials and Methods

2.1. Materials, Reagents, and Instrumentations

BFS (SEM image in Figure 1, JEOL-7800F, Jeol, Tokyo, Japan) used herein was obtained from a steel making company in South Korea; slag was milled, and powders with a mesh size of below 200 were collected. As reported in previous studies utilizing BFS [2,30], crystal phases of BFS were not observed by XRD analysis (Analytical X-ray B.V.X'pert-MPD, Philips, EA Almelo, The Netherlands; scanning range of 3° – 70° (2θ) ($\text{CuK}\alpha$) using a step size of 0.02° (2θ) at 40 kV/40 mA). The concentrations of elements in oxide compounds were quantitatively measured by X-ray fluorescence (XRF; MXF-2400, Shimadzu, Kyoto, Japan, approximately 1 g of a sample was used to make a glass disc with 5.5 g of $\text{Li}_2\text{B}_4\text{O}_7$ as the flux) for the estimation of the leaching ratio (LCH. R) of metal ions from BFS by using AR.

AR was freshly prepared before each experiment, due to its rapid decomposition; for the preparation of 30, 60, 90, 120, and 150 mL of AR, AR was prepared at a volume ratio of 3:1 of hydrochloric acid (HCl , >32%, Fluka, St. Louis, MO, USA):nitric acid (HNO_3 , 60%–61%, Junsei, Tokyo, Japan). In addition, 2 mL of perchloric acid (HClO_4 , 70%, Junsei) was added in AR because HClO_4 is widely used for the oxidation of Na and K during wet chemical analysis. The actual molar ratio of HCl to HNO_3 was 2.4:1. DI water (Milli-Q Gradient-A10, Millipore, Billerica, MA, USA) of 270, 240, 210, 180, and 150 g was added to AR, affording 10%, 20%, 30%, 40%, and 50% AR solutions, respectively. The corresponding molar concentrations of the diluted AR solutions (300 mL) were 1.12, 2.23, 3.35, 4.47, and 5.59 M. The metal ion concentration was measured by inductively coupled plasma optical emission spectroscopy (ICP-OES, Optima 5300 DV, Perkin-Elmer, Waltham, MA, USA, relative standard deviation <3%).

2.2. Leaching Procedures

In the experiments, 20, 25, and 30 g BFS were used for comparing the effect of the variation of L/S on the leaching of metal ions. According to the experimental procedure shown in Figure 1, first, an aliquot of BFS was dispersed in a certain amount of DI water at 343 K by overhead stirring. Second, a specific concentration of freshly prepared AR was added to the suspension, and stirring was continued for the desired reaction time. Within several minutes, the color of this mixture changed from bright brown to yellow as the reaction proceeded, and the mixture appeared to be very sticky (this observation is hypothesized to correspond to gel formation). Gelation started within 10 min of the experiment, which was maintained until the reaction was stopped. Finally, at time intervals shown in Figure 1 during the experiment, approximately 10–15 mL of the gel was removed from the mixture and filtered using a $0.45\ \mu\text{m}$ membrane (mixed cellulose acetate membrane, Advantec, Tokyo, Japan). The metal ion concentration was quantified by ICP-OES. As a control experiment for comparing the effects of AR on the leaching of Si and metal ions from BFS, leaching was conducted using boiling DI water. For this purpose, 30 g of slag was dispersed in boiling DI water for 2 h, followed by boiling and stirring. The concentrations of Ca, Mg, Fe, Mn, Al, Ti, and Si as measured by ICP-OES were 56, 0.01, 0.01, 0.01, 2.2, 0, and 19 mg/L, respectively, indicating that boiling water does not affect the leaching of metal ions (compared with the concentrations of the metal oxides present in raw BFS shown in Table 1).

All leaching procedures were completed within 2 h. After the completion of experiments, the gelled slag-AR mixtures were separated using a glass microfiber filter (GF/C, Whatman, Brentford, UK) into an aqueous phase and a solid phase. Experiments for the comparison of L/S ratios were conducted using 20 and 25 g BFS per 20% of the AR solution by identical leaching procedures. After filtration, the solid phase was washed with DI water until the pH of the phase was approximately neutral, as tested by a pH paper. Finally, the solid phase was dried in an oven at 348 K, which was further used for X-ray diffraction (XRD) analysis, as well as for specific surface area measurement by Brunauer, Emmett, and Teller (BET) analysis using six adsorption data points at $P/P_0 = 0.05, 0.1, 0.15, 0.2, 0.25,$

and 0.3 (Quadrasorb-SI, Quantachrome, Boynton Beach, FL, USA, N₂ adsorption, 1.5–2 g sample was used for each analysis).

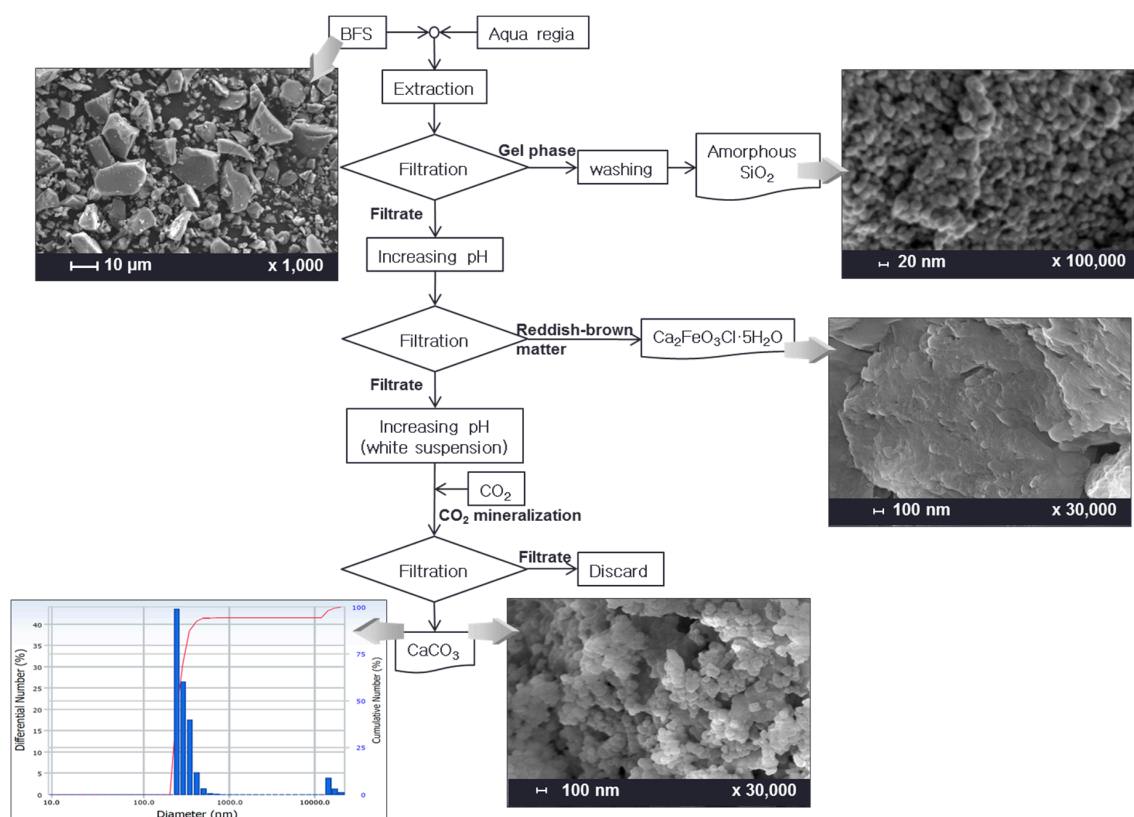


Figure 1. Experimental procedures and SEM images of BFS and precipitates.

A 5 M NaOH solution (Samchun Chemicals, Seoul, Korea) was added to the collected aqueous phase for increasing the pH up to 12 while continuously monitoring the pH of the filtrate using an Orion pH meter (3 Star Plus), followed by the bubbling of CO₂ gas (99.999%, Gasco, Asan, Korea). The collected precipitates were identified by XRD. Figure 1 shows the experimental procedures. Particle size of CaCO₃ was measured by dynamic light scattering (DLS, ELSZ-1000, Otsuka Electronics, Osaka, Japan). All averaged values and standard deviations were obtained from triplicate experiments.

3. Results and Discussion

It is imperative to know the chemical composition of BFS before conducting experiments for the comparison and estimation of the leaching efficiency (LCH. R) of metal ions from BFS under the given experimental conditions. Table 1 summarizes the results obtained from the quantitative measurement of Si and metal oxides present in BFS. The concentrations of the main components CaO, SiO₂, and Al₂O₃ were 44, 35, and 12 wt %, respectively. On the other hand, the concentrations of other metal oxides, such as FeO, MgO, TiO, and MnO, were less than 10 wt %. Table 2 summarizes the elemental concentrations of Si and metal ions (mg/kg), calculated using the values shown in Table 1. These values were used as “reference values” for estimating the LCH. Rs of Si and other metal ions from the slag by AR treatment.

Table 1. Concentrations of metal oxides (wt %) present in BFS by XRF analysis.

Component	SiO ₂	Al ₂ O ₃	Fe ₂ O ₃	CaO	MgO	K ₂ O	Na ₂ O	TiO ₂	MnO	P ₂ O ₅	Loss on Ignition
%	35.24	12.33	2.01	43.63	4.13	0.18	0.33	0.44	0.23	0.01	−1.14

Alkaline-earth metal ions primarily react with carbonated CO₂ during CO₂ mineralization. In this study, Ca or Mg present in BFS was exploited; typically, pure Ca and Mg carbonates are white; however, marginal amounts of Fe can render them reddish-yellow. Even though Si and Al were present in BFS at a significantly high concentration, they do not form their respective carbonates via CO₂ mineralization. Nevertheless, they can still be retained as impurities within Ca or Mg carbonates during the formation of carbonate minerals by CO₂ mineralization. Consequently, it is valuable to separate Si from slag because high-purity Si can be used in industrial applications, such as in semiconductors or solar cells. Furthermore, a mixture of Si and Al can also be used for producing absorbents [23]. Ca and Mg carbonates with fewer impurities can result in increased market values of CO₂ mineralization.

3.1. Effect of the Variation of AR Solution Concentration and Leaching Time on Leaching Efficiency

The AR–BFS mixture was stirred while simultaneously removing 10–15 mL aliquots of the mixture at a certain leaching interval, followed by filtration for measuring the concentrations of seven elements (Table 2) by ICP-OES. It is difficult to perform filtration, attributed to the silica-gel phase in the mixture [31]. The concentrations measured by ICP-OES (dimension: mg/L) were converted into the weight (dimension: mg) of the elements in a mixture of the AR solution and BFS. It was crucial to convert dimension because the results in Table 2 could not be directly compared with those obtained by ICP-OES.

Table 2. Concentration of elements (mg/kg) in BFS (calculated by XRF results from Table 1).

Element	Si	Al	Fe	Ca	Mg	K	Na	Ti	Mn	P
mg/kg	164,758	65,273	14,061	311,876	24,913	1494	2449	2638	1782	44

LCH. R is defined as follows [32]:

$$\text{LCH. R} = \frac{(\text{concentration of each element measured by ICP – OES}) \times (\text{volume of the mixture})}{(\text{concentration of each element measured by XRF}) \times (\text{weight of BFS})}$$

Figure 2 shows the LCH. R of each element when the AR solution concentration was varied from 10% to 50%, corresponding to (A)–(E), respectively. As shown in Figure 2, a 10% AR solution (A) leached 70% of Ca and Mg from the raw slag after a leaching time of 2 h, 60% of Mn, and 20% of Fe; however, Al and Ti were not leached. The Si concentration decreased from 7% to nearly 0% as leaching proceeded. As shown in Figure 2B, 20% AR leached all Ca and Mg, as well as greater than 90% of Mn. It also leached 80% and 40% of Al and Fe, respectively. Nevertheless, it was difficult to dissolve Ti in 20% AR. The concentration of Si in the filtered liquid phase decreased from 12% to nearly 0%. Moreover, when 30% AR was used (Figure 2C), a large standard deviation of the averaged value from triplicate experiments was observed for Fe and Ti. Even though leaching experiments were performed in triplicate, the reason for the peculiar decrease of the Ti concentration after 20 min was not known. The rate of change in the Si concentration was similar to that with the use of 10% AR. The concentration change of Ca, Mg, and Mn was similar to that with the use of 20% AR. In contrast, the dissolved concentrations of Fe, Al, and Ti increased to nearly 100%, 100%, and 50%, respectively. Increase in the AR concentration to 40% (Figure 2D) resulted in the increase of the dissolved concentrations of Ca, Mg, Fe, Mn, and Al from the early stage of leaching. Figure 2E shows the results obtained with the use of 50% AR. The leaching experiment had to be stopped in 30 min because the filtration of the mixture into liquid and solid phases was not possible by vacuum filtration. The Ca and Al concentrations reached 100% with the use of 40% AR. However, the dissolved Mg, Fe, and Mn concentrations slightly decreased as compared with those obtained with the use of 40% AR.

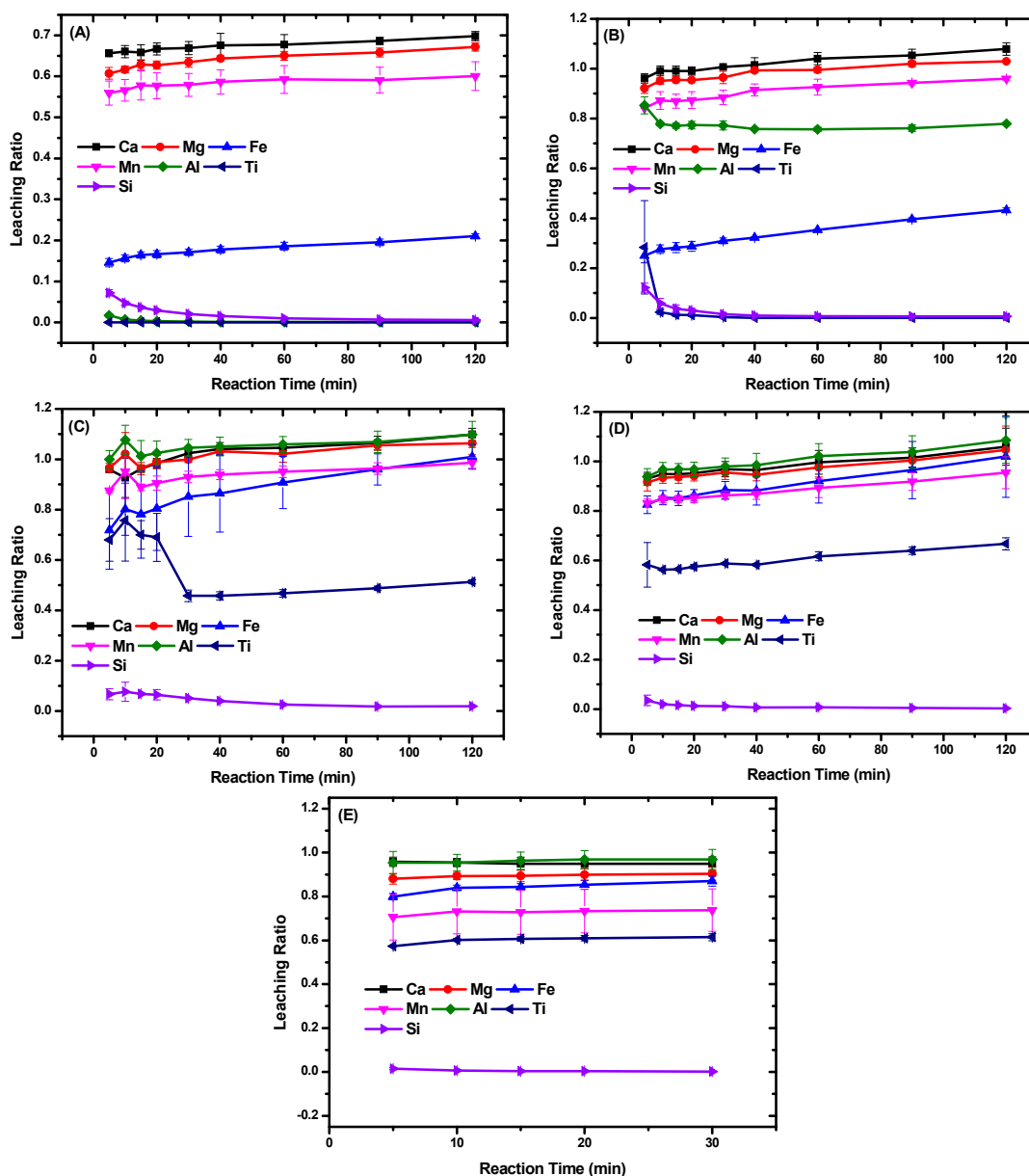


Figure 2. Effect of the variation in the AR concentrations of (A) 10%; (B) 20%; (C) 30%; (D) 40%; and (E) 50% with BFS suspended in DI water on the leaching ratio (LCH. R.).

With increasing AR concentration, the leaching ratio of metal ions increased with time. However, the concentration of leached Si decreased or did not change with time. This observation is hypothesized to be due to the decomposition of the amorphous silica phase (actually BFS itself) when metal ions present in BFS are leached by contact with the AR solution; as a result, the amorphous silica phase is converted to hydrophilic silanol (Si–O–H) [33], which results in the loosening of the silica-gel-phase structure; this loosening of the structure results in the free movement of Mg ions in the liquid phase.

In Figure 2, the five graphs indicate that the time required to attain a steady state of leaching efficiency (not relevant to the degree of leaching) decreases with increasing AR concentration. The maximum leaching efficiency was attained with a slag-50% AR mixture. High AR concentrations are clearly advantageous for reaching a steady state of leaching time. However, the isolation of alkaline-earth metal ions for CO₂ mineralization and exclusion of impurities, such as Fe- and Mn-coloring carbonate minerals, should be considered: this consideration may increase the feasibility of CO₂ mineralization for producing relatively high-purity carbonate minerals. Leaching efficiencies

were compared at a specific time (assuming the steady state in terms of Si concentration). The steady state for the LCH. R of Si was achieved in 20 min with the use of 10% AR. Above this concentration, no significant fluctuation in leaching efficiency was observed within 20 min. Hence, the leaching efficiency of each element is compared at 20 min, and Figure 3 shows the results obtained from comparison. The LCH. Rs of all elements were not affected by the AR concentration, except for those obtained using 10% AR. In addition, the LCH. R of iron was low with the use of 20% AR, confirmed by the ICP-OES results. Table 3 shows the selectivity of each metal ion present in BFS by the equation below using the results from Figure 3.

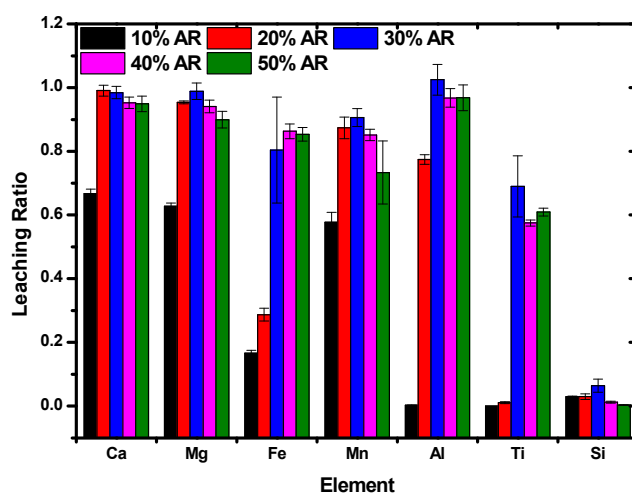


Figure 3. Comparison of the leaching ratio (LCH. R) of elements corresponding to the AR concentration at a leaching time of 20 min.

Table 3. Selectivity of elements from leaching experiments.

AR Concentrations (%)	Ca	Mg	Fe	Mn	Al	Ti	Si
10	32	30	8	28	0	0	1
20	25	24	7	22	20	0	1
30	18	18	15	17	19	13	1
40	18	18	17	16	19	11	0
50	19	18	17	15	19	12	0

$$\text{Elemental selectivity (\%)} = \frac{\text{concentration of each element}}{\sum (\text{concentration of seven elements})} \times 100 \quad (1)$$

The values obtained by the above equation were calculated from the results shown in Figure 3. For leaching a specific element, it is crucial to estimate the optimum AR concentration. Table 3 shows the results obtained. The selectivities of Ca and Mg increased with the use of 10% AR, as well as that of Mn. With the use of 20% AR, the selectivities of Ca and Mg decreased; as compared with an AR concentration of greater than or equal to 30%, 20% AR was advantageous for deselecting Fe. The results from Table 3 and Figure 3 suggested that 20% AR is optimum for CO₂ mineralization in terms of both LCH. R and selectivity. Increasing acid concentration clearly resulted in increased amounts of the leached metal elements. In CO₂ mineralization, the amounts of leached Ca and Mg for the formation of carbonate minerals need to increase, while those of Fe- and Mn-coloring carbonate minerals and Si as impurities need to decrease. For CO₂ mineralization, the filtrate obtained from acid by leaching is subjected to alkali agents (e.g., NaOH) for increasing the reactivity of CO₂ at high pH (i.e., pH swing) [8,27–29]. Hence, the acid concentration needs to be rationally chosen for CO₂ mineralization. In our experiments, with respect to leaching Ca and un-leaching Fe, 20% AR was appropriate to obtain white CaCO₃ by CO₂ mineralization.

3.2. Effects of the Liquid-to-Solid Ratio on Leaching Efficiency

From the previous section, 20% of AR is confirmed to be optimum for leaching metal ions for CO₂ mineralization with the use of 30 g slag and a 300 mL acid solution. This section deals with experiments involving the comparison of L/S. The AR concentration and AR solution volume were maintained constant; only, the weight of BFS suspended in the AR solution was changed: 20 and 25 g. The use of slag with a weight greater than 30 g (i.e., 32 g) was not appropriate because significantly harder and sticky gels led to the inefficient filtration of the filtrate from the gel. The variation of LCH. Rs was observed. Figure 4 shows the results obtained. The highest LCH. R was obtained with the use of 20 g slag (a similar result was obtained with the use of 40% AR with 30 g slag shown in Figure 4B). First, the observed LCH. R of Si, corresponding to an impurity for CO₂ mineralization, was 66%, which then decreased to 40% at the final stage with large deviation (Although we have conducted several additional experiments, the reason for this significant deviation is not clear at this time). With the decrease in the slag weight for leaching experiments, the amount of filter cake also significantly decreased (Figure 4D) because Si included in the slag was dissolved with the other six elements present in the AR solution; hence, silica gel is not formed, as observed in the panel of Figure 4D. The LCH. Rs of Fe, Al, and Ti were similar to that of Si, implying that these metals are caged in the silica gel. On the other hand, Ca, Mg, and Mn were released, irrespective of silica-gel formation. Bao et al. [32] have reported that by increasing L/S from 10 to 15, the leaching ratios of Ca and Mg increase to approximately 75% and 35%, respectively. In contrast, the experiments conducted herein using AR did not show significant differences in the LCH. Rs of Ca, Mg, and Mn. However, the LCH. Rs of Fe, Al, Ti, and Si were affected by L/S (L/S: 0.3/0.02; 10, 0.3/0.025; 12, and 0.3/0.3; 15).

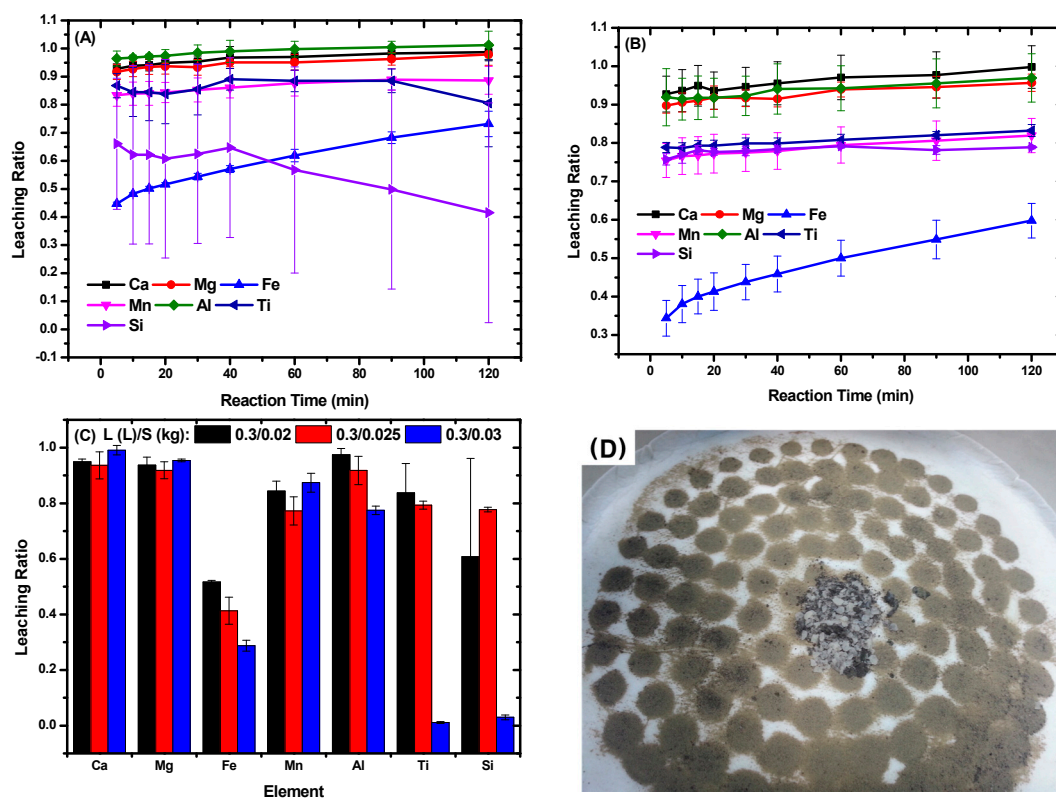


Figure 4. Effects of the variation in the weight of BFS of (A) 20 and (B) 25 g in a 20% AR solution (300 mL) on the leaching ratio (LCH. R) of elements. Graph (C) denotes the comparison of the leached ratio of elements corresponding to the ratio of slag weight (g) to AR (20%) liquid volume (mL) of 20/300, 25/300, and 30/300 at a leaching time of 20 min. Picture (D) represents the residue washed with DI water upon filtration after a leaching time of 120 min with 25 g slag/300 mL at 20% AR.

It is hypothesized that the use of acetic acid for leaching metals from slag results in the formation of a silica gel harder than that obtained using AR even with similar L/S. At 120 min, the concentrations of Fe in the filtrates were 686 ± 42 , 701 ± 53 , and 608 ± 13 mg/L for 20, 25, and 30 g slag, respectively. The optimum L/S is possibly 0.3/0.03 (L/kg), caused by the high LCH. Rs of Ca and Mg, as well as low LCH. Rs of Fe, Ti, and Si, despite the fact that filtration was slow, attributed to silica-gel formation. After filtration, the solid phase separated from the mixture of AR and BFS was collected. The solid phase was washed with DI water until the pH of the phase increased to approximately neutral pH, as confirmed by a pH paper. This solid phase was dried in an oven at 348 K and then gently milled. In Section 3.1, we stated that the gelled-slag phase predominantly consisted of an amorphous hydrophilic silanol phase, which was not supposed to change after acid treatment and drying. Figure 5 shows the XRD patterns of the dried amorphous powder and raw BFS. Broad signals centered at around 23° were observed, which was in agreement with data reported by Rohilla et al. [34]. In addition, XRF analysis was employed to quantify the oxide compounds of the treated powder and raw BFS. AR treatment possibly afforded highly pure amorphous silica powder (shown in the SEM image in Figure 1) with a large specific surface area, implying fine size. Table 4 briefly summarizes these results. After AR-DI water treatment, almost all metal ions included in raw BFS were removed, resulting in a high-purity amorphous silica phase. With increasing AR concentration, the purity of silica increased up to 90% [35]. Hence, the purity of the silica phase increases up to 99%, caused by the loss on ignition primarily caused by adsorbed water. With increasing AR concentration, the measured specific surface area of the AR-DI water-treated powder also increased. The results obtained from measurements of XRF and specific surface area indicated that the AR-DI water treatment renders utility to BFS in terms of a high-purity material and an adsorbent. According to the experiments, the L/S should be optimized to obtain silica powder from BFS besides CO_2 mineralization.

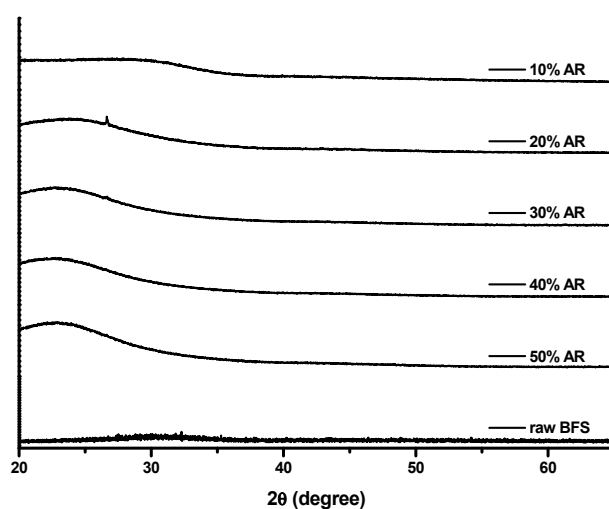


Figure 5. XRD patterns of the separated solid phase treated by AR-DI water and raw BFS.

Table 4. Oxide compounds found in BFS treated by AR-DI water as well as their specific surface areas.

AR Conc. (%)	SiO ₂ (%)	Al ₂ O ₃ (%)	Fe ₂ O ₃ (%)	CaO (%)	MgO (%)	K ₂ O (%)	Na ₂ O (%)	TiO ₂ (%)	MnO (%)	P ₂ O ₅ (%)	Loss on Ignition (%)	Specific Surfaces Area (m ² /g)
10	46.30	16.60	1.89	23.78	2.00	0.21	0.12	0.51	0.13	0.02	−8.92	24.9
20	71.97	6.75	3.10	3.4	0.32	0.11	0.01	0.96	0.03	0.02	−12.48	250.8
30	89.15	0.12	0.18	<0.01	0.04	0.01	<0.02	0.59	<0.01	<0.01	−9.59	692.6
40	90.95	0.09	0.04	0.01	0.04	0.01	<0.02	0.29	<0.01	<0.01	−8.75	751.3
50	90.49	0.15	0.07	0.15	0.05	0.01	<0.02	0.32	<0.01	<0.01	−8.83	696.5

3.3. CO₂ Mineralization of Ca Leached from BFS

In previous sections, 20% AR is confirmed to be the optimum concentration as it affords high leaching ratios of Ca and Mg and high rejection ratios of other elements. The carbonation of the filtrate obtained using 20% AR with CO₂ was briefly conducted.

Before the addition of NaOH, the pH of the filtrate was 3.15. First, 5 M NaOH was added into the filtrate for slowly increasing pH. Next, when a pH of around 7.5 was attained, a reddish-brown cloudy substance was observed, which was filtered for XRD characterization; the precipitate was Ca₂FeO₃Cl·5H₂O (JCPDS 00-044-0445, above pattern and photograph in Figure 6). Figure 1 also shows its SEM image. Additional NaOH was added into the filtered liquid for increasing pH. At a pH of 10.5, a white precipitate was suspended in the liquid, which was used for reaction with 200 mL/min of CO₂ while monitoring pH. CO₂ was continuously bubbled using an air diffuser (circular, 3 cm in diameter) until the pH of the suspension was decreased to be constant at around 7.5. Then, the suspension was filtered, affording a white precipitate; the crystal phase of this precipitate by XRD was found to be CaCO₃ (JCPDS 01-081-2027 (calcite), 00-041-1475 (aragonite), and 01-085-0849 (calcite); second pattern and photograph in Figure 6). Figure 1 also shows a magnified SEM image and particle size distribution (near 320 nm) of CaCO₃. ICP-OES analysis was performed for estimating the elemental concentration of Ca₂FeO₃Cl·5H₂O and CaCO₃ to corroborate the results obtained from XRD analysis. Table 5 shows the results. The Si concentrations of those two precipitates were below the detection limit, indicating that Si is already collected as an amorphous silica phase by leaching (Figure 1). Substantial amounts of Mg, Mn, and Al in Ca₂FeO₃Cl·5H₂O were measured, but the elements did not form crystals. In addition, even though the CaCO₃ precipitate consisted of a large amount of Mn, Mn-doped crystals (e.g., Mn·Ca(CO₃)₂) or MnCO₃ was not formed in the three CaCO₃ crystal phases. The CaCO₃ obtained herein can be utilized as an industrial material, e.g., as a paper-making filler, because the shape and size distribution of the obtained CaCO₃ herein can enhance the smoothness of paper surfaces, as well as printing quality [36]. Other metal ions, such as Mg, Al, and Ti were not supposed to form crystalline minerals. Hence, with the stepwise increase in the pH of the filtrate, impurities were eliminated from the CaCO₃ crystal lattice, affording white CaCO₃.

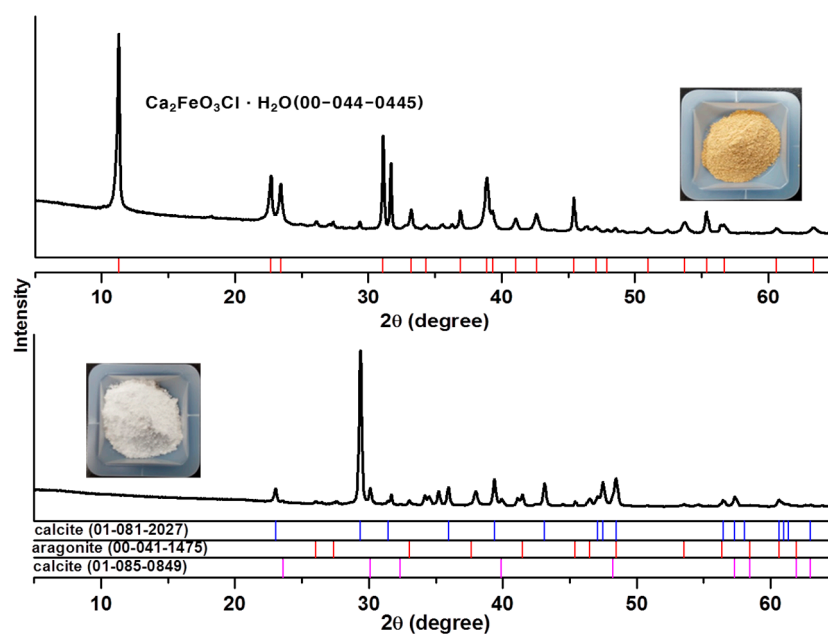


Figure 6. XRD patterns of reddish-brown and white precipitates with increasing pH of the filtrate obtained by the reaction of 20% AR. Magnified photographs of two powders from Figure 1 are also shown.

Table 5. Analysis methods and elemental concentrations of the precipitates formed with increasing pH of the filtrate with 20% AR.

XRD		ICP-OES (mg/kg)						
Phase	JCPDS	Si	Fe	Mg	Mn	Al	Ti	Ca
Ca ₂ FeO ₃ Cl·5H ₂ O	00-044-0445	<0.28	-	34,299	349,590	121,300	<0.05	732,486
CaCO ₃ (calcite)	01-081-2027							
CaCO ₃ (aragonite)	00-041-1475	<0.28	<0.12	1.1	143,636	205	<0.05	-
CaCO ₃ (calcite)	01-085-0849							

4. Conclusions

In this study, alkaline-earth metal ions and other metal ions present in BFS were leached using AR for CO₂ mineralization. The effects of the variation in the AR concentration and L/S ratio on the leaching efficiencies of alkaline-earth metal ions, such as Ca and Mg, were investigated for decreasing leaching ratios of other metal ions such as Fe. The AR concentration was varied from 10% to 50% for controlling the LCH. Rs of metal ions present in slag, which could increase the purity of carbonate minerals formed by CO₂ mineralization. An optimum concentration of 20% AR was required for increasing the leaching of Ca and Mg while simultaneously decreasing the leaching of Fe, Al, and Ti. An optimum L/S of 0.3/0.03 (=10) at 20% AR was required for decreasing the leaching of Fe, Ti, and Si; moreover, the leaching of Ca and Mg was not significantly different at other L/S values. Si can retain metal ions, such as Fe, during its hydration (by forming silica gel), indicating that silica gel affects leaching selectivity. Preventing silica-gel formation by adjusting L/S adversely affects the purity of carbonate minerals, which is in agreement with the results reported by Crom et al. [30]. Impurities retained in the silica gel phase, such as Fe, Mn, and Al, were removed by washing with deionized water, affording a high-purity (~99%) amorphous silica powder with a wide specific surface area (several hundred meter square per gram).

By this study, BFS treated by AR was confirmed to be useful for CO₂ mineralization in terms of producing high-purity CaCO₃ for industrially useful materials as fillers for paper making and for capturing CO₂ materials via the Ca-looping cycle [37]. Amorphous silica powder can be used for preparing semiconductors, as well as an adsorbent for various potential applications [29], e.g., dehumidification and elimination of toxic matter. To increase the feasibility of the study conducted herein, economic evaluation in terms of carbonate mineralization [35] with CaCO₃, amorphous silica, and reuse of AR will be conducted in a future study.

Acknowledgments: This study was supported by the Basic Research Project of the Korea Institute of Geoscience and Mineral Resources (KIGAM), funded by the Ministry of Science, Information and Communication Technologies ICT, and Future Planning.

Author Contributions: Jun-Hwan Bang and Soochun Chae conceived and designed the experiments; Jun-Hwan Bang and Seung-Woo Lee performed the experiments and analyzed the data; Chiwan Jeon, Kyungsun Song, Sangwon Park, Whan Joo Jo contributed reagents, materials, and analysis tools; and Jun-Hwan Bang wrote the paper.

Conflicts of Interest: The authors declare no conflict of interest.

References

1. Lackner, K.S.; Wendt, C.H.; Butt, D.P.; Joyce, E.L.; Sharp, D.H. Carbon dioxide disposal in carbonate minerals. *Energy* **1995**, *20*, 1153–1170. [[CrossRef](#)]
2. Teir, S.; Eloneva, S.; Fogelholm, C.J.; Zevenhoven, R. Dissolution of steelmaking slags in acetic acid for precipitated calcium carbonate production. *Energy* **2007**, *32*, 528–539. [[CrossRef](#)]
3. Bobicki, E.R.; Liu, Q.; Xu, Z.; Zeng, H. Carbon capture and storage using alkaline industrial wastes. *Prog. Energy Combust. Sci.* **2012**, *38*, 302–320. [[CrossRef](#)]
4. Lackner, K.S.; Butt, D.P.; Wendt, C.H. Progress on binding CO₂ in mineral substrates. *Energy Convers. Manag.* **1997**, *38*, S259–S264. [[CrossRef](#)]

5. Sanna, A.; Dri, M.; Hall, M.R.; Maroto-Valer, M. Waste materials for carbon capture and storage by mineralization (CCSM)—A UK perspective. *Appl. Energy* **2012**, *99*, 545–554. [[CrossRef](#)]
6. Bang, J.-H.; Jang, Y.N.; Kim, W.; Song, K.S.; Jeon, C.W. Precipitation of calcium carbonate by carbon dioxide microbubbles. *Chem. Eng. J.* **2011**, *174*, 413–420. [[CrossRef](#)]
7. Leung, D.; Caramanna, G.; Maroto-Valer, M. An overview of current status of carbon dioxide capture and storage technologies. *Renew. Sust. Energy Rev.* **2014**, *39*, 426–443. [[CrossRef](#)]
8. Azdarpour, A.; Asadullah, M.; Mohammadian, E.; Hamidi, H.; Junin, R.; Karaei, M.A. A review on carbon dioxide mineral carbonation through pH-swing process. *Chem. Eng. J.* **2015**, *279*, 615–630. [[CrossRef](#)]
9. Boot-Handford, M.E.; Abanades, J.C.; Anthony, E.J.; Blunt, M.J.; Brandani, S.; Dowell, N.M.; Fernández, J.R.; Ferrari, M.C.; Gross, R.; Hallett, J.P.; et al. Carbon capture and storage update. *Energy Environ. Sci.* **2014**, *7*, 130–189. [[CrossRef](#)]
10. Power, I.M.; Harrison, A.L.; Dipple, G.M.; Wilson, S.A.; Kelemen, P.B.; Hitch, M.; Southam, G. Carbon Mineralization: From natural analogues to engineered systems. *Rev. Miner. Geochem.* **2013**, *77*, 305–360. [[CrossRef](#)]
11. Eloneva, S.; Said, A.; Fogellholm, C.J.; Zevenhoven, R. Preliminary assessment of a method utilizing carbon dioxide and steelmaking slags to produce precipitated calcium carbonate. *Appl. Energy* **2012**, *90*, 329–334. [[CrossRef](#)]
12. Kleiv, R.A.; Thornhill, M. Mechanical activation of olivine. *Miner. Eng.* **2006**, *19*, 340–347. [[CrossRef](#)]
13. Huijgen, W.J.; Witkamp, G.J.; Comans, R.N. Mechanisms of aqueous wollastonite carbonation as a possible CO₂ sequestration process. *Chem. Eng. Sci.* **2006**, *61*, 4242–4251. [[CrossRef](#)]
14. Nduagu, E.; Björklöf, T.; Fagerlund, J.; Wärnå, J.; Geerlings, H.; Zevenhoven, R. Production of magnesium hydroxide from magnesium silicate for the purpose of CO₂ mineralisation—Part 1: Application to Finnish serpentinite. *Miner. Eng.* **2012**, *30*, 75–86. [[CrossRef](#)]
15. Nduagu, E.; Björklöf, T.; Fagerlund, J.; Mäkilä, E.; Salonen, J.; Geerlings, H.; Zevenhoven, R. Production of magnesium hydroxide from magnesium silicate for the purpose of CO₂ mineralisation—Part 2: Mg extraction modeling and application to different Mg silicate rocks. *Miner. Eng.* **2012**, *30*, 87–94. [[CrossRef](#)]
16. Ferrini, V.; De Vito, C.; Mignardi, S. Synthesis of nesquehonite by reaction of gaseous CO₂ with Mg chloride solution: Its potential role in the sequestration of carbon dioxide. *J. Hazard. Mater.* **2009**, *168*, 832–837. [[CrossRef](#)] [[PubMed](#)]
17. Ballirano, P.; De Vito, C.; Ferrini, V.; Mignardi, S. The thermal behaviour and structural stability of nesquehonite, MgCO₃·3H₂O, evaluated by in situ laboratory parallel-beam X-ray powder diffraction: New constraints on CO₂ sequestration within minerals. *J. Hazard. Mater.* **2010**, *178*, 522–528. [[CrossRef](#)] [[PubMed](#)]
18. Glasser, F.P.; Jauffret, G.; Morrison, J.; Galvez-Martos, J.-L.; Patterson, N.; Imbabi, M.S.-E. Sequestering CO₂ by mineralization into useful nesquehonite-based products. *Front. Energy Res.* **2016**, *4*, 1–7. [[CrossRef](#)]
19. Morrison, J.; Jauffret, G.; Galvez-Martos, J.L.; Glasser, F.P. Magnesium-based cements for CO₂ capture and utilization. *Cem. Concr. Res.* **2016**, *85*, 183–191. [[CrossRef](#)]
20. Ballirano, P.; De Vito, C.; Mignardi, S.; Ferrini, V. Phase transitions in the Mg-CO₂-H₂O system and thermal decomposition of dypingite, Mg₅(CO₃)₄(OH)₂·5H₂O: Implications for geosequestration of carbon dioxide. *Chem. Geol.* **2013**, *340*, 59–67. [[CrossRef](#)]
21. Hopkinson, L.; Kristova, P.; Rutt, K.; Cressey, G. Phase transitions in the system MgO-CO₂-H₂O during CO₂ degassing of Mg-bearing nsolutions. *Geochim. Cosmochim. Acta* **2012**, *76*, 1–13. [[CrossRef](#)]
22. Eloneva, S.; Teir, S.; Salminen, J.; Fogelholm, C.J. Fixation of CO₂ by carbonating calcium derived from blast furnace slag. *Energy* **2008**, *33*, 1461–1467. [[CrossRef](#)]
23. Chiang, Y.W.; Santos, R.M.; Elsen, J.; Meesschaert, B.; Zevenhoven, R. Towards zero-waste mineral carbon sequestration via two-way valorization of ironmaking slag. *Chem. Eng. J.* **2004**, *249*, 260–269. [[CrossRef](#)]
24. Hall, C.; Large, D.J.; Adderley, B.; West, H.M. Calcium leaching from waste steelmaking slag: Significance of leachate chemistry and effects on slag grain mineralogy. *Miner. Eng.* **2014**, *65*, 156–162. [[CrossRef](#)]
25. Eloneva, S.; Puheloinen, E.M.; Kanerva, J.; Ekroos, A.; Zevenhoven, R.; Fogelholm, C.-J. Co-utilisation of CO₂ and steelmaking slags for production of pure CaCO₃—Legislative issues. *J. Clean. Prod.* **2010**, *18*, 1833–1839. [[CrossRef](#)]
26. Lee, S.; Kim, J.W.; Chae, S.; Bang, J.-H.; Lee, S.W. CO₂ sequestration technology through mineral carbonation: An extraction and carbonation of blast slag. *J. CO₂ Util.* **2016**, *1*, 336–345. [[CrossRef](#)]

27. Kodama, S.; Nishimoto, T.; Yamamoto, N.; Yogo, K. Development of a new pH-swing CO₂ mineralization process with a recyclable reaction solution. *Energy* **2008**, *33*, 776–784. [[CrossRef](#)]
28. Azdarpour, A.; Asadullah, M.; Mohammadian, E.; Junin, R.; Hamidi, H.; Manan, M.; Daud, A.R. Mineral carbonation of red gypsum via pH-swing process: Effect of CO₂ pressure on the efficiency and products characteristics. *Chem. Eng. J.* **2015**, *264*, 425–436. [[CrossRef](#)]
29. Sanna, A.; Dri, M.; Maroto-Valer, M. Carbon dioxide capture and storage by pH swing aqueous mineralisation using a mixture of ammonium salts and antigorite source. *Fuel* **2013**, *114*, 153–161. [[CrossRef](#)]
30. Crom, K.D.; Chiang, Y.W.; Gerven, T.V.; Santos, R.M. Purification of slag-derived leachate and selective carbonation for high-quality precipitated calcium carbonate synthesis. *Chem. Eng. Res. Des.* **2015**, *104*, 180–190. [[CrossRef](#)]
31. Qin, W.; Li, W.; Lan, Z.; Qiu, G. Simulated small-scale pilot plant heap leaching of low-grade oxide zinc ore with integrated selective leaching of zinc. *Miner. Eng.* **2007**, *20*, 694–700. [[CrossRef](#)]
32. Bao, W.; Li, H.; Zhang, Y. Selective leaching of steelmaking slag for indirect CO₂ mineral sequestration. *Indus. Eng. Chem. Res.* **2010**, *49*, 2055–2063. [[CrossRef](#)]
33. Greenberg, S.A.; Jarnutowski, R.; Chang, T.N. The behavior of polysilicic acid. II. The rheology of silica suspensions. *J. Colloid Sci.* **1965**, *20*, 20–43. [[CrossRef](#)]
34. Rohilla, S.; Kumar, S.; Aghamkar, P.; Sunder, S.; Agarwal, A. Investigation on structural and magnetic properties of cobalt ferrite/silica nanocomposites prepared by the coprecipitation method. *J. Magn. Mater.* **2011**, *32*, 897–902. [[CrossRef](#)]
35. Sanna, A.; Hall, M.; Maroto-Valer, M. Post-processing pathways in carbon capture and storage by mineral carbonation (CCSM) towards the introduction of carbon neutral materials. *Energy Environ. Sci.* **2012**, *5*, 7781–7796. [[CrossRef](#)]
36. Bang, J.-H.; Song, K.; Park, S.; Jeon, C.W.; Lee, S.-W.; Kim, W. Effect of CO₂ bubble size, CO₂ flow rate and calcium source on the size and specific surface area of CaCO₃ particles. *Energies* **2015**, *8*, 12304–12313. [[CrossRef](#)]
37. Miranda-Pizarro, J.; Perejón, A.; Valverde, J.M.; Sánchez-Jiménez, P.E.; Pérez-Maqueda, L.A. Use of steel slag for CO₂ capture under realistic calcium-looping conditions. *RSC Adv.* **2016**, *6*, 37656–37663. [[CrossRef](#)]



© 2016 by the authors; licensee MDPI, Basel, Switzerland. This article is an open access article distributed under the terms and conditions of the Creative Commons Attribution (CC-BY) license (<http://creativecommons.org/licenses/by/4.0/>).